Seismic Hazard Determination for the Coastal Region of South China I*: Generic Crustal Modelling

Nelson Lam[1], Adrian Chandler[2], John Wilson[3], and Graham Hutchinson[4]

1. Senior Research Fellow and Senior Lecturer, Department of Civil and Environmental Engineering, The University of Melbourne, Parkville, Victoria, 3052, Australia
2. Professor, Department of Civil Engineering, The University of Hong Kong, Pokfulam Road, Hong Kong, Special Administrative Region, China
3. Senior Lecturer, Department of Civil and Environmental Engineering, The University of Melbourne, Parkville, Victoria, 3052, Australia
4. Professor of Civil Engineering and Head of Civil and Environmental Engineering Dept., The University of Melbourne, Parkville, Victoria, 3052, Australia

ABSTRACT: *The objective of this paper is to describe and illustrate a rational seismological modelling approach for developing design earthquake response spectra for application in a moderate seismicity region. In the first stage a seismicity model is developed, using the Coastal Region of South China (CRSC) as an example. Combining this with a generic source model and an assumed generic crustal model, the ground motion parameters (representing acceleration, velocity and displacement properties) have been determined. Importantly, the generic crustal model is assumed to have properties which are identical to the continental shield region of Eastern North America (ENA). Subsequently, response spectrum modelling procedures are described and applied to the example region, to determine design-level spectra for rock sites. The response spectra predicted by the seismological model were found to be very consistent with current code provisions, and with design spectra proposed by other researchers, in the velocity-controlled medium period range. However, significant discrepancies have been identified in other period ranges. The ground motion parameters and response spectra derived in this study were based on the generic ENA crustal conditions. The effects which the regional crustal properties and the crustal thickness have upon the ground motion parameters have been described in the second part of the paper.*

Keywords: Seismic hazard; Earthquake ground motion; Response spectrum; Seismological model; Acceleration; Velocity; Displacement; South China; Hong Kong

1. INTRODUCTION

A number of major Chinese cities with strategic and regional economical significance, including Hong Kong, Shen Zhen, Macau, Guangzhou (provincial capital city of Guangdong), Yangjiang, and Shantou are located along the Coastal Region of South China (CRSC). Over the past 900 years, approximately one earthquake every 20-25 years with Magnitude 5 or larger has been recorded in the region. All such earthquakes have occurred in a source area of approximately 400,000 square kilometers which straddles across the South China coastline as shown in Figure 1 [1, 2]. Five events exceeded magnitude M7 and eleven events exceeded magnitude M6, amongst the records. The largest events have occurred in the Shantou

area, NE of Hong Kong, with four recorded earthquakes with $M > 7$, the last being a M7.4 event in the Taiwan Straits in 1994 which was felt throughout the South China region [2]. The potential threat to lives and properties of the unprepared communities in the region from such moderate seismicity has been a growing concern in recent years.

A few areal source zones in the region have been analysed [1-5]. Earthquakes occurring within each zone were assumed to occur at random, and not along specifically identified fault lines. The zonation was largely based on the distribution and the completeness of pre-instrumental (historical) records, whilst tectonic considerations were used as references. Information obtained from these seismicity studies has further been used as input to
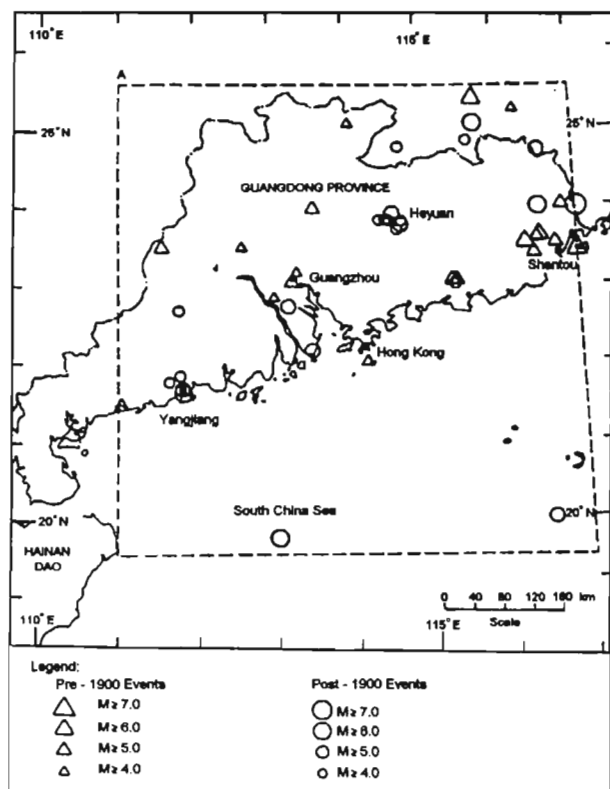
Figure 1. Map of the coastal region of South China (after Ref. [1]).

conventional probabilistic seismic hazard analyses (involving Cornell-McGuire Integration [6]) to predict the peak ground accelerations (PGA) in probabilistic terms [1, 4, 5]. The PGA has been used accordingly to scale a normalised acceleration response spectrum for engineering applications [4]. Both the attenuation model and the normalised response spectrum model adopted in these studies were originally developed for Eastern North America (ENA), and in particular the north-east United States (US). This approach was based on the view that South China and ENA have a number of significant similarities in terms of seismic hazard since both are intraplate regions which are remote from tectonic plate boundaries. However, there is in fact no rational basis to assume that earthquake ground motion properties in all intraplate regions are similar.

A more rational approach to seismic hazard prediction is to attempt to model the velocity, acceleration and displacement parameters which represent ground motion properties over the entire frequency domain. Such ground motion parameters have been modelled by researchers for different regions across South China, using methods which combine seismic Intensity (I) attenuation relationships and ground motion attenuation relationships developed for Western North America, WNA (notably California) with Intensity attenuation relationships developed from indigenous isoseismal data [7, 8]. The reliability and limitations of these methods in deriving ground motion attenuation relationships have been thoroughly reviewed in the second part of the paper [9].

The seismic hazard predictive methodologies described above each contain a great deal of uncertainty, resulting from the notable lack of information concerning the seismicity in the region as well as from over-simplified assumptions associated with the link between seismicity (level of seismic activity) and seismic hazard (level of ground shaking).

An alternative methodology has been developed and applied in this paper to address the uncertainties just described. The procedure has particular advantages in areas of low to moderate seismicity where both the seismicity data and indigenous strong motion data are scarce. Importantly, the procedure was evolved within the framework of a seismological model which has been developed in the United States over the last 20 years to rationalize ground motion simulations [10-13]. The authors' review of the seismological model has been provided in References [14, 15].

A generic displacement response spectrum model developed recently by the authors is founded on the fundamental relationship between seismic moment and the maximum displacement at the ground surface. The predicted displacements have been shown to be in good agreement with those obtained from empirical models developed in WNA and in Europe [16]. The displacement response spectrum model has been further developed into a comprehensive response spectrum model. Again, the velocity and the acceleration predictions have been shown to be in good agreement with a number of existing empirical models [17].

The seismic hazard evaluation procedure introduced in the present paper has been formulated using the response spectrum models just described. A significant feature of the procedure is that the earthquake source effects and the crustal modification effects on the ground motions may be modelled separately in two stages. In Stage One, seismicity information is input into the procedure to model the source effects (refer Section 2), whilst a generic crustal model based directly on ENA geological conditions has been considered in Stage Two to model the crustal effects (Section 3). The ENA generic crustal model is thereby assumed to be applicable to other regions of low to moderate seismicity, such as the study region comprising the CRSC. The significance and reliability of this assumption has been systematically tested in the second part of the paper [9], which develops a regional crustal model for the CRSC, using localised geological information from South China.

The ground motion parameters adopted in Stage Three of the modelling procedure (Section 4) are (I) Effective Peak Ground Displacement (EPGD), (II) Effective Peak Ground Velocity (EPGV) and (III) Effective Peak Ground Acceleration (EPGA). These parameters are then combined in Stage Four of the procedure to construct the displacement and the acceleration response spectra which define the seismic hazard over a wide range of structural natural period [refer Section 5]. The derived response spectra have

then been compared with the design response spectrum recommended by Scott et al in Reference [4] and the response spectrum provisions of the Chinese earthquake code [18], for the CRSC. Discrepancies between the response spectra predictions in the critical period ranges for civil engineering structures have been identified. In order to test the theory that the accurate modelling of regional crustal effects has an important influence on spectral predictions, the second part of the paper [9] presents a thorough review of regional geological properties for the CRSC and recomputes the response spectral model by including crustal modifications that are specific to the region. The second part of the paper also discusses the uncertainty issues arising from these studies, as mentioned above, with reference to both the conventional and the alternative proposed modelling procedures for deriving regional design response spectra for implementation in earthquake resistant design codes and associated procedures.

The effect of soils overlying bedrock on ground motions (site effects) is not considered in this paper. Similarly, the uncertainties associated with the modelling of the response of infrastructure and building components to the defined hazard (as represented by the elastic design response spectrum) is also outside the scope of consideration in the present paper.

2. SOURCE MODELLING (STAGE ONE)

2.1. Seismicity and M-R Combinations

The properties of direct seismic shear waves generated at the source of an earthquake are controlled by two parameters: (I) The seismic moment or the Moment Magnitude which determines the amount of energy released by the fault rupture, and (II) The stress drop (measured in bars) which determines the rate of energy release and hence the frequency content of the generated waves.

The Moment Magnitude (M) at any given distance from the site (R) can be determined probabilistically [19], in accordance with the seismicity of the various identified source zones surrounding the site. Source zone configurations can be very complex in high seismicity areas. In contrast, source zones in low and moderate seismicity regions, which are generally free of distinct major active faults, are often arbitrarily defined from broad geographical or seismological considerations, and they are sometimes known as seismotectonic provinces within which earthquakes are assumed to occur at random [20, 21]. A given site is usually located within one such large areal source zone, in which the level of uniform seismicity may be defined by the Richter-Gutenberg magnitude recurrence relationship:

$$log_{10} N(M) = a - bM \qquad (1a)$$

where $N(M)$ may be defined as the expected number of earthquakes of Magnitude, M, or greater which occur

within an area of $100,000 \ km^2$ over a 100 year period.

Alternatively,

$$log_{10} N(M) = a_5 - b(M - 5) \qquad (1b)$$

where a_5 is the logarithm of the total number of earthquakes with magnitude 5 or greater.

In regions of low and moderate seismicity where source zones are difficult to define reliably, the assumption of uniform seismicity is not unreasonable. The Moment Magnitude-Distance (M-R) combination may be expressed as a probabilistic function of the seismicity of the source zone. The number of earthquakes, N^*, generated within a circular area, S' (with a radius R_s), within a source zone surrounding a given site, is proportional to the size of that area (πR_s^2) and the average return period, T_{RP} (years). Hence, $N(M)$ can be defined by the following relationship (based on proportionality):

$$N^* = N(M)(\pi R_s^2 T_{RP})(100 \ years \times 100,000 \ km^2) \qquad (2)$$

A specific source area $S' = \pi R_s^2 (km^2)$ is needed to produce one event, that is $N^* = 1$, of magnitude M or larger, in a period of T_{RP} (years). Hence the design earthquake magnitude, M, for given values of R_s, a_5 and b can be determined by substituting Eq. (2), $N^* = 1$, into Eq. (1b), and rearranging the terms as follows:

$$M = 5 + \left\{ log_{10} (\pi R_s^2 T_{RP}) - 7 + a_5 \right\} / b \qquad (3)$$

We now ask at what average distance R the epicenter of an event of magnitude M or larger would occur, measured from a point site that floats in the open-ended region characterized by seismicity parameters a_5 and b. Expressing the total area S' in terms of a median-probability (50 - percentile) distance R, one obtains [19]:

$$\pi R^2 = \pi R_s^2 / 2 = S' / 2 \qquad (4)$$

Hence

$$R = R_s / \sqrt{2} \qquad (5)$$

Thus, Eq. (3) can be rewritten as follows:

$$M = 5 + \left\{ log_{10} (2\pi R^2 T_{RP}) - 7 + a_5 \right\} / b \qquad (6)$$

For a given design return period and seismicity parameters a_5 and b, Eq. (6) may be used to determine an appropriate set of uniquely defined design M-R combinations, for seismic hazard evaluation purposes. In Section 2.2 below, such M-R combinations have been derived for the Coastal Region of South China based on local seismicity parameters.

2.2. Seismicity of the Coastal Region of South China (CRSC)

There have been 119 earthquakes recorded in the Coastal Region of South China (CRSC) with magnitude M greater

than or equal to 4.75, since 1067 A.D. These include eighty four events with magnitudes between $M4.75$ and $M5.25$, twenty one between $M5.5$ and $M5.75$, seven between $M6.0$ and four between $M6.75$ and $M7.0$ and five between $M7.3$ and $M7.5$. The region local to Hong Kong had relatively fewer recorded events [1].

To compare published recurrence relationships for the CRSC, three key studies of the region's seismicity have been considered, namely those by Lee et al [1], Chan and Zhao [22] and Wong et al [3]. The regions studied in the seismic catalogues of the above 3 studies were quite simi-lar, as shown in Figure 2. The source zone model studied in Reference [1] covered the largest area, and this was split into the Inner and the Outer seismic source zones which have been identified as Source Zones A and D, respec-tively, in Figure 2a. In contrast, the so-called Reduced Zone considered in Reference [22] focused on a much smaller area surrounding Hong Kong and has been identified as Source Zone B in Figure 2b. Similarly, Source Zone S2 defined in Reference [3] has been identified as Source Zone C in Figure 2c. In computing the areas of the source zones considered, 1 degree of latitude has been assigned a distance of 113km and 1 degree of longitude a distance of 105km, as appropriate for the overall latitude and longi-tude of the region. Table 1 summarises the key recurrence-related data from the 3 studies, employing the normalised form of Eqs. (1a and 1b), along with the earthquake records database used in each study.

It is noted from Table 1 that Source Zones C and D produced similar predictions, in that they are categorised by very small b-values implying a relatively high probabil-ity of occurrence for larger magnitude events. In contrast, Source Zone B has the highest b-value, which implies higher probability for smaller magnitude earthquakes within the considered range $M2.0$ - $M6.0$. Source Zone A produced predictions which lie between those of the other researchers. The apparent differences between these

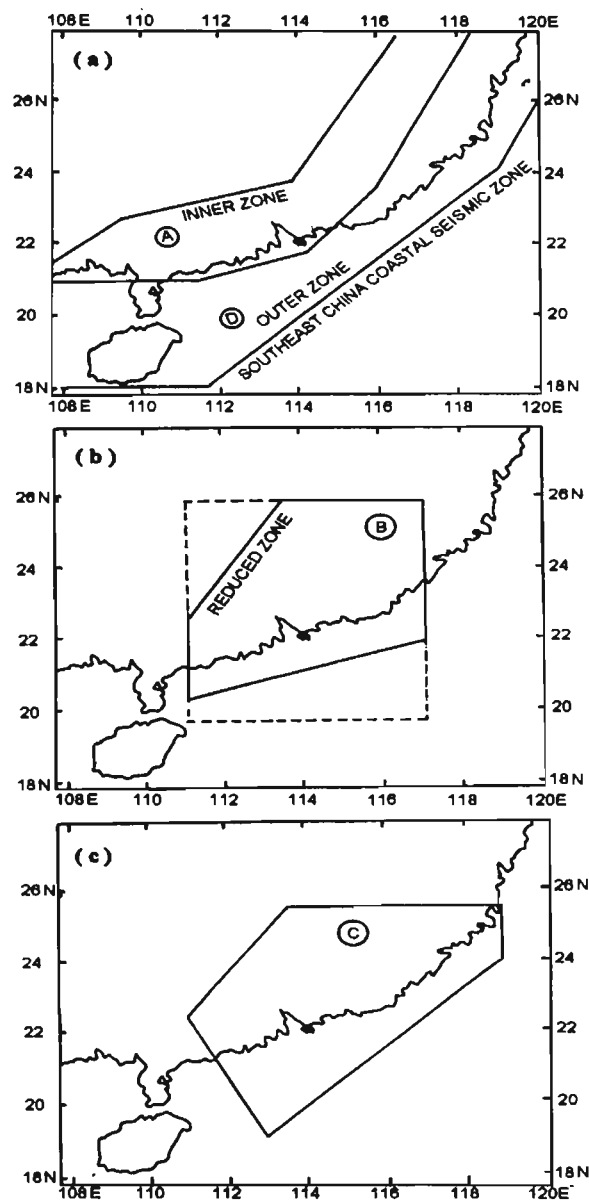**Figure 2.** Alternative source zone models for the South China region.

Table 1. Seismicity Parameters Summary.

Source Zone	Origin of Data	a	a_s	b	Source Area (km²)	No. of Records	Remarks
A	C.F. Lee et al (Inner Zone)[2]	4.93	0.83	0.82	230,000	36	16 records with M>5 and only 3 records with M>6
B	L.S. Chan et al (Reduced Zone)[22]	5.54	1.14	0.88	255,000	5233	Only 44 records with M>4
C	Y.L. Wong et al (Zone S2)[3]	4.28	0.88	0.68	356,000	128	
D	C.F. Lee et al (Outer Zone)[2]	4.35	1.00	0.67	260,000	55	33 records with M>5 and 10 records with M>6

models are the result of the varying definitions of the source areas, along with differences between the associated databases of earthquake records.

The M-R combinations derived from the magnitude-recurrence relationships described above have been listed in Tables 2a-2c for average return periods of 500, 1000 and 2500 years, which correspond to a 10%, 5% and 2% probability of exceedance, respectively, during an exposure period of 50 years.

Table 2a. M-R combinations for 500 years return period.

| R (km) | Moment Magnitude M | | | |
	Source Model A	Source Model B	Source Model C	Source Model D
10	4.2	4.6*	4.3	4.3
20	4.9	5.3*	5.1	5.1
30	5.3	5.7	5.7	5.7*
50	5.9	6.2	6.3	6.3*

Table 2b. M-R combinations for 1000 years return period.

| R (km) | Moment Magnitude M | | | |
	Source Model A	Source Model B	Source Model C	Source Model D
10	4.5	5.0*	4.5	4.7
20	5.3	5.6*	5.6	5.6
30	5.7	6.0	5.9	6.1*
50	6.3	6.5	6.6	6.8*

Table 2c. M-R combinations for 2500 years return period.

| R (km) | Moment Magnitude M | | | |
	Source Model A	Source Model B	Source Model C	Source Model D
10	5.0	5.4*	5.1	5.3
20	5.8	6.1*	6.0	6.1
30	6.2	6.5	6.5	6.7*
50	6.7	7.0	7.2	7.3*

* Note: Critical M-R combinations.

Clearly, Source Model D (b=0.67) predicts the most critical M-R combinations for distances $R \geq 30km$, whereas Source Model B (b=0.88) predicts the most critical M-R combinations for smaller distances. The critical M-R combinations based on the collection of models have been summarised in Table 3a.

The M-R combinations considered here are associated with distances ranging between 10-50km, and this

Table 3a. Critical M-R combinations (M<7).

| R | Moment Magnitude M | | |
	T_{RP}=500 years	T_{RP}=1000 years	T_{RP}=2500 years
10	4.6	5.0	5.4
20	5.3	5.6	6.1
30	5.7	6.1	6.7
50	6.3	6.8	(7.3)

corresponds to Moment Magnitudes ranging approximately between M=5 and M=7. The latter has been tentatively taken as the moment magnitude of the maximum credible event (MCE) and corresponds to the largest MCE magnitude adopted in earlier probabilistic studies of the region's seismicity [1, 3, 4, 5]. However, as mentioned above, a small number of earthquakes exceeding Magnitude 7.0 have been recorded historically in the CRSC, but their epicenters have all been located in the Shantou or Hainan Island areas (see Figure 1), located on the periphery of the CRSC region and distant from its major urban centres, as listed in Section 1. Nevertheless, because of the uncertainty surrounding the appropriate MCE magnitude, a sensitivity study has been carried out to determine the effect of an increased MCE on the computed seismic hazard, as reported and discussed in the second part of the paper [9]. The M-R combinations shown in Table 3a are augmented by the M-R combinations associated with M=7, as given in Table 3b.

Table 3b. Critical M-R combinations (M=7).

| M | R (km) | | |
	T_{RP}=500 years	T_{RP}=1000 years	T_{RP}=2500 years
7(MCE)	85	60	40

3. GENERIC CRUSTAL MODELS (STAGE TWO)

3.1. Introduction to Crustal Effects

According to the seismological model, three major types of mechanism will significantly modify the amplitude and frequency content of the seismic shear waves along their travel path from source to site, and they are: (i) Crustal Amplification (ii) Anelastic Attenuation and (iii) Geometrical Attenuation. Each of these mechanisms are briefly described in the following sub-sections.

3.1.1. Crustal Amplification

The crustal amplification of the seismic shear waves along their path is made up of the following components: (a) Mid-crust amplification and (b) Upper crust amplification.

Mid-crust amplification occurs only close to the

earthquake source, and the amount of amplification depends on the density (ρ_s) and the shear wave velocity (β_s) of the earth's crust at the depth of the source (normally depth >5km). An average amplification factor of 1.3 has been identified in Western North America (WNA) [12] and 1.0 (no amplification) in Eastern North America (ENA) [15].

Upper crust amplification is associated with the variation of the shear wave velocity with depth (as defined by the shear wave velocity profile) according to the principle of conservation of energy [23]. Generally, large shear wave amplification is associated with very low shear wave velocity of the earth's crust near the ground surface. The amplification is also dependent on the length of the transmitted shear waves, and this selective amplification process can modify the frequency content as well as the amplitude of the upward propagating waves [15, 24]. This frequency dependent amplification function can be determined from a representative shear wave velocity profile which shows the increase in the shear wave velocity of the earth's crust with increasing depth. However, determining such a profile can be difficult since the shear wave velocity is typically required over a large depth. Thus, for convenience, the average shear wave velocity within the top 30m of the earth crust (β_{30}) has been recommended [24] to be the reference shear wave velocity in identifying and representing the profile.

According to the "Quarter Wavelength Approximation" [24], the periods (T_{amp}) of the amplified sinusoidal components of the upward propagating shear waves can be related to the reference depth (x) by the following expression:

$$T_{amp} = 4x / \beta_x \qquad (7)$$

where x is the reference depth, β_x is the average shear wave velocity of the earth's crust within the reference depth, and T_{amp} is the upper period limit of the sinusoidal components which can be amplified within this reference depth.

Natural periods of engineering interest for normal structures typically range between 0.2 seconds and 2 seconds, with longer periods in the range 2 to 4 seconds being associated with tall buildings and long-span bridges. The periods 0.2 seconds and 2 seconds associated with the lower band correspond respectively to x=30m and x=1000m, according to Eq. (7) [assuming $\beta_x = 600m / sec$ for the top 30m and $\beta_x = 2000m / sec$ for the top 1000m]. Thus, shear wave velocity information within the recommended reference depth of 30m only indicates amplification of wave components pertaining to very short periods (less than or equal to 0.2 seconds). Recent investigations have identified that sinusoidal components in the period range of 2-3 hertz (i.e. 0.3-0.5 seconds) are most affected by upper crust amplifications [24], and this corresponds roughly to a reference depth in the range 100-300m, depending on

the assumed average shear wave velocity, Clearly, the earth's crust in the top 30m is not sufficiently representative of the overall amplification effects in an engineering context.

The 30m depth could well be a convenient reference level from the point of view of collating data obtained from wave propagation studies conducted in shallow boreholes. However, such an advantage is clearly irrelevant in regions such as South China where downhole (or uphole) data is not the primary source of shear wave velocity information. Further, geology at shallow depths less than 100-200m is typically subjected to weathering and deposition, which vary significantly between localities. Using the deeper crust as reference would reduce the variability and hence give a better representation of regional properties. Based on the above considerations, the authors recommend that the reference shear wave velocity be defined in accordance with a reference depth of at least 100m (and preferably 200m) instead of 30m.

3.1.2. Anelastic Attenuation

Seismic shear waves are attenuated depending on the wave transmission quality of the earth's crust, as defined by the Quality Factor (Q). The dimensionless factor Q is normally expressed in the following form:

$$Q = Q_0 (f / f_0)^n \qquad (8)$$

where Q_0 and n are regional dependent coefficients, f is the frequency of the wave component, and $f_0 = 1\mathrm{Hz}$.

Anelastic attenuation is associated with the dissipation of energy in the bedrock medium, and hence it increases with the number of wave cycles. The result in higher frequency waves are more susceptible to attenuation than lower frequency waves, since the number of wave cycles for any given travel path increases with frequency. In principle, such attenuation increases with distance from the source. However, in "young and heavily folded" crustal regions, the wave transmission quality of the earth's crust in the top 3-4km can be distinctly poorer than the same at greater depths [24, 25]. Most of the attenuation thus occurs very close to the earth's surface, and consequently, the observed effects appear distant independent. For computational convenience, the effect of such upper crust attenuation has normally been separated from that of the whole path anelastic attenuation.

Upper crust attenuation has been observed in California which is both geologically and tectonically active [12, 24], and in Southeastern Australia which is geologically active but tectonically stable [15, 25].

The upper crust attenuation can be defined by the single parameter κ (kappa) which may be related to the Quality Factor of the upper crust (Q_{uc}), as follows:

$$\kappa = R_{uc} / (Q_{uc} \beta_{uc}) \qquad (9)$$

where R_{uc}, Q_{uc} and β_{uc} are the depth, the quality factor,

and the average shear wave velocity, respectively, of the upper crust possessing a distinctively lower shear wave transmission quality.

3.1.3. Geometrical Attenuation

Seismic shear waves are attenuated as the wavefronts propagate and extend from the source. In an elastic full space, such geometrical attenuation is associated with spherical spreading. As the wavefront reaches the ground surface, free surface amplification occurs as a result of waves rebounding from the free surface. Both the spherical attenuation and free-surface amplification have been incorporated in the "source" model presented in Section 2 (although they are strictly "path" mechanisms).

Close to the source, ground motions are mainly contributed by direct body waves which comprise compressive waves and shear waves. At a certain distance from the source, direct body waves reaching the ground surface coincide with body waves reflected from the Moho discontinuity, as shown in Figure 3. The superimposition of the two waves has been found to result in little overall attenuation of ground motions over a significant distance. The modelling of the attenuation characteristics of seismic shear waves from distant earthquakes are particularly relevant to seismic hazard evaluation in low and moderate seismicity regions, such as South China. A tri-linear attenuation model developed to model the above effects is presented as follows [14]:

$$G = R_0 / R \qquad \text{for } R < 1.5D$$
spherical attenuation (10a)

$$G = R_0 / 1.5D \qquad \text{for } 1.5D < R < 2.5D$$
zero attenuation (10b)

$$G = (R_0 / 1.5D)\sqrt{(2.5D / R)} \qquad \text{for } R > 2.5D$$
cylindrical attenuation (10c)

where $D=$ *thickness* of the earth crust (in *km*) measured to the Moho-discontinuity, and $R_0 = 1km$.

("Tri-linear" refers to linear functions in the logarithmic scale).

3.2. Crustal Classifications

Two generic crustal models have been defined in accordance with the average bedrock properties observed in ENA and WNA. These are the generic "Hard Rock" model and the generic "Rock" model, respectively [14-16, 24]. The crustal parameters identified with these models have been listed in Table 4.

The features of earthquake ground motions in regions characterised by the "Hard Rock" and the "Rock" conditions lead to very different ground motion characteristics, and this has important engineering implication. In particular, the frequency contents of ground motions compatible with the two generic models are significantly different. The "Hard Rock" model typically gives ground motions which
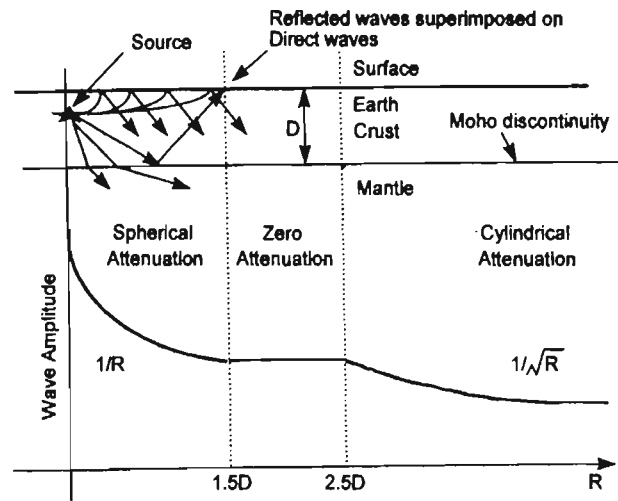

Figure 3. Geometrical attenuation of seismic shear waves.

have higher spectral accelerations in the short period range. The "Rock" model, on the other hand, tends to feature lower short-period spectral accelerations. The effects the crustal models have upon spectral response quantities such as displacement, velocity and acceleration have been described in detail in the second part of the paper [9].

The generic hard rock crustal model (typified by the ENA parameters) is generally considered characteristic of continental stable shield regions such as Eastern North America (ENA), Western Australia and Eastern Europe. In contrast, the generic rock crustal model (typified by the WNA parameters) is considered characteristic of the younger, folded geological formations such as those existing in California, Eastern Australia, parts of Middle East, Southern Europe, South America and Northern China. Significantly, this geological distinction is not always well correlated with the seismo-tectonic classification of the region (namely "inter-plate" versus "intra-plate" regions). For the subject region of South China (CRSC), geological information [26] indicates that, whilst not strictly a stable shield area (due to the somewhat higher level of seismic activity recorded over the past 500,000 years compared, for example, with ENA), the region may be considered to have crustal wave transmission characteristics which generically match those of ENA and other stable shield regions. Further discussion of this point has been provided in the second part of the paper [9].

The crustal thickness (D) depends on the region and is not defined by the generic crustal model. The significant effects of D over the seismic hazard level are evident in the tri-linear attenuation relationship described in Section 3.1.3. and in Figure 3. Continental crustal thickness varies between 30-70km [27]. In ENA, D=50km has been assumed [13]. The same value of D has been adopted in the analyses described in this paper to predict the attenuation of seismic shear waves in CRSC. Consequently, spherical attenuation has been assumed for all the M-R combinations considered in Tables 3a and 3b, since the limit of 1.5D is 75km, Eq. (10a). In other words, the effects of "zero

Table 4. Parameters of the generic crustal models.

Path Parameters	Associated Mechanisms	Generic "Hard Rock" Model	Generic "Rock" Model
ρ_s (at depth of source)	Mid-Crust Amplification	2800kg/m^3	2700kg/m^3
β_s (at depth of source)	Mid-Crust Amplification	3800m/sec	3500m/sec
β_{100} (at 100m depth)	Upper Crust Amplification	2850m/sec (refer Figure 4)	1400m/sec (refer Figure 4)
Q_0	Anelastic Whole Path Attenuation	680	204
n	Anelastic Whole Path Attenuation	0.36	0.56
κ	Upper Crust Attenuation	0secs	0.35 - 0.050secs

Note: The shear wave velocity profiles associated with these generic models are shown in Figure 4.
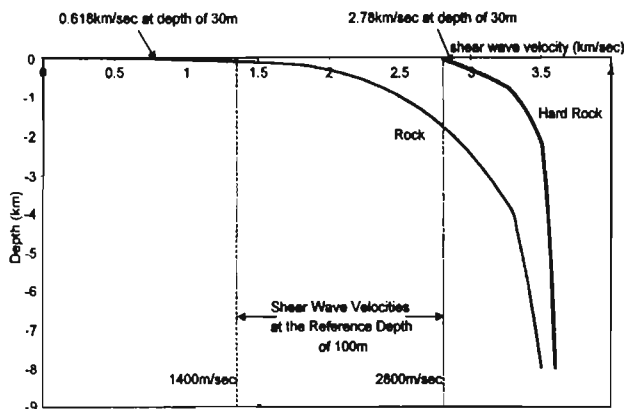
Figure 4. Shear wave velocity profiles of the generic crustal models.

attenuation" and "cylindrical attenuation" have been assumed to be insignificant within the distance range of interest. The actual regional crustal thickness can be determined by surface wave dispersion analyses of teleseismic records [28]. The effects the regional crustal properties have upon the ground motion parameters are considered in Reference [9], and are outside the scope of this paper which predicts ground motion parameters strictly in accordance with the assumption of ENA conditions.

4. GROUND MOTION PARAMETER PREDICTIONS (STAGE THREE)

In sections 4.1. and 4.2. below, spectral parameters related to peak ground displacement and velocity have been predicted in accordance with results obtained from Seismological Model simulation studies undertaken recently by the authors [16, 17]. In the first instance, only the properties of the seismic shear waves generated at the earthquake source have been modelled whilst modification of the frequency content along the wave travel path is addressed in the second part of the paper [9]. This is justified, since the conventional spherical attenuation and free surface amplification effects have been built-in to the "Source" model. Thus, the displacement and velocity ground motion parameters predicted by the source model alone (Sections 4.1 and 4.2) will be representative of surface motions provided that the earth's crust possesses excellent wave transmission properties. This is the case in continental shield regions, for example ENA, which in this paper has been assumed in developing a generic crustal model for the CRSC as discussed in Section 3, above. However, the prediction of ground accelerations has been deferred to Section 4.3, since high frequency ground motion components are significantly affected by attenuation, under most crustal conditions.

4.1. Displacement Parameter Predictions

The peak ground displacement (PGD) is predominantly determined by the Magnitude-Distance (M-R) combination, according to recent simulation studies [16, 17]. The PGD is intended to indicate the maximum displacement demand of very long period structures or structures experiencing significant lengthening of their effective natural period as a result of ductile yielding. However, PGD has been found to be overly conservative for predictions associated with very large magnitude earthquakes in that the displacement demand can saturate at an effective natural period well over 10 seconds, which is seldom attained in reality. The alternative displacement parameter, as introduced recently by the authors, is termed the Effective Peak Ground Displacement (EPGD) and is defined as the response spectral displacement of a single-degree-of-freedom oscillator possessing a natural period of 5 seconds and 5% damping. Thus, EPGD is more representative of the displacement threshold of engineering structures than PGD. Note, EPGD is only moderately affected by crustal and source stress drop conditions [17], unlike the PGD.

The following expression has been developed by the

authors [16, 17] to predict the EPGD parameter:

$$EPGD\,(mm) = 14\,\{0.20 + 0.80\,(M-5)^{2.3}\}\,(30/R) \qquad (11)$$

for $R \geq 10km$.

Predictions using Eq. (11) have been presented in References [16, 17]. These have been shown to be in excellent agreement with predictions obtained in accordance with Ambrasey's spectral attenuation relationship developed from European seismological data [29, 30].

The EPGD's predicted using Eq. (11), for the critical M-R Combinations (summarized in Table 3), are given in Table 5.

Tables 5a-5c: Effective peak ground displacement (EPGD) predictions.

(a) 500 years return period

R(km)	M	EPGD (mm)
10	4.6	(see footnote)
20	5.3	5
30	5.7	8
50	6.3	14
85	7.0 (MCE)	20

Note: The predicted displacement for a M=4.6 earthquake is considered to have little engineering significance and has therefore been omitted.

(b) 1000 years return period

R(km)	M	EPGD (mm)
10	5.0	8
20	5.6	9
30	6.1	17
50	6.8	28
60	7.0 (MCE)	29

(c) 2500 years return period

R(km)	M	EPGD (mm)
10	5.4	12
20	6.1	25
30	6.7	41
40	7.0 (MCE)	43

4.2. Velocity Parameter Predictions

The relationship between ground velocity and ground displacement depends on the frequency content of the generated seismic shear waves which in turn is a function of (i) The Moment Magnitude (M) of the earthquake and (ii) The stress drop properties which are related to the rate of energy release at the source.

Stress drop is highly variable and is difficult to predict as the underlying factors governing its behaviour are as

yet not fully understood. Recorded stress drops in earthquakes range from below 30 bars to over 500 bars.

Observations from intraplate (ENA) earthquake records indicate an average stress drop of around 100-200 bars [10, 14, 15, 31] which are significantly higher than for WNA, where stress drops vary with the earthquake magnitude from 50 bars (M=7.5) to 120 bars (M=5.5) [12, 14, 15].

However, neither the average Fourier amplitude source spectra (as presented in the above-cited seismology references) nor the average response spectra derived from the seismological model simulations [16], suggest any significant difference in the average source frequency properties of seismic shear waves generated by earthquakes in the seemingly different seismo-tectonic regions of Eastern and Western North America (ENA and WNA, respectively). The different frequency properties of earthquake ground motions observed at the ground surface are therefore considered to be largely attributed to crustal modifications [9].

The generic ENA source model originally developed by Atkinson [10], which is slightly more conservative than its WNA counterpart, appears to be suitable for adoption in low and moderate seismicity regions, including the subject region addressed in this study.

Seismological model simulations by the authors [16, 17] have also derived the following expression for the EPGV:

$$EPGV\,(mm/sec) = 50\,\{\,0.35 + 0.65\,(M-5)^{1.8}\}\,(30/R) \qquad (12)$$

for $R \geq 10km$

The EPGV's predicted using Eq. (12), for the critical M-R Combinations (summarized in Tables 3a and 3b), are given in Table 6.

Tables 6a-6c: Effective peak ground velocity (EPGV) predictions.

(a) 500 years return period

R(km)	M	EPGV(mm/sec)
10	4.6	(see footnote)
20	5.3	32
30	5.7	35
50	6.3	42
85	7.0 (MCE)	46

Note: The predicted velocity for a M=4.6 earthquake is considered to have little engineering significance and has therefore been omitted.

(b) 1000 years return period

R(km)	M	EPGV(mm/sec)
10	5.0	53
20	5.6	46
30	6.1	56
50	6.8	67
60	7.0 (MCE)	65

(c) 2500 years return period

R(km)	M	EPGV(mm/sec)
10	5.4	71
20	6.1	84
30	6.7	102
40	7.0 (MCE)	98

The resulting V/D (EPGV/EPGD) ratios are highly magnitude dependent, and their values are listed in Table 7. Clearly, the larger the earthquake magnitude, the lower the V/D ratio. Note, this ratio is unaffected by the assumed spherical attenuation and hence it is independent of distance, R.

Table 7. V/D ratios.

Moment Magnitude	V/D (secs^{-1})
5	6.0*
5.5	5.0*
6	3.5
6.5	2.5
7	2.0

* The V/D ratio can be very sensitive to rounding off errors associated with both the modelling of the EPGD and EPGV, particularly for small magnitude events.

The very high wave transmission quality of the rocks in (i) continental shield regions covered by very old sedimentary rocks or metamorphic rocks or (ii) in regions covered by crystalline rocks formed by massive volcanic intrusion such as granite, will preserve most of the medium and low frequency components of the seismic shear waves generated at the source of the earthquake. Hence, whilst the EPGD, EPGV and V/D predictions shown in Tables 5-7, respectively, relate specifically to the Coastal Region of South China (CRSC), similar values are expected from earthquakes in other regions with comparable crustal properties.

4.3. Modifications to the Acceleration Parameter

The high frequency properties of the seismic shear waves are known to be very sensitive to anelastic attenuation. In the generic "Hard Rock" crustal model, anelastic attenuation is moderate and is uniformly distributed along the wave travel path. Seismological simulations by the authors for such crustal conditions [17] have derived the A/V (EPGA/EPGV) ratios which are dependent on both M and R, as shown in Table 8, and by the following expression:

$$A/V\,[\,g\,/(m\,/\,sec)] = 6 + (30 - R)\{3 + 0.15\,(M - 5)\}\,/\,90$$

$$+ 1.2\,(6 - M) \qquad (13)$$

The A/V ratio is shown to increase from 3 to 8 (depending on the earthquake magnitude and distance), which is generally very high compared with previous observations on rock sites cited in References [32, 33]. Such high A/V ratios are attributed to the excellent wave transmission quality of the "Hard Rock" crust in ENA. Near field earthquake ground motions recorded instrumentally in this region and similar regions (such as South China) are very rare, and hence similar A/V ratios are seldom observed from strong motion data. It is noted that the Chicultimi Nord earthquake records of the 1988 Saguenay earthquake event (in Quebec, Canada) indicate an A/V ratio in the order of 5 at a distance of approximately 43km from the source (of magnitude 6), which is in general agreement with the recommended values in Table 8.

Table 8. Magnitude and distance dependent A/V ratios for generic "Hard Rock" model [Units:g/(m/sec)].

M	R=10km	R=30km	R=50km	R=85km
5	8.0	7.0	6.5	5.5
5.5	7.5	6.5	6.0	4.5
6	6.5	6.0	5.5	4.0
6.5	6.0	5.5	4.5	3.5
7	5.5	5.0	4.0	3.0

Similar simulations for the generic "Rock" model have also been carried out by the authors and presented in Reference [17]. The A/V ratios of the relatively "softer" rock were substantially lower due to upper crust amplification and attenuation occurring close to the ground surface. The derived A/V ratios defined by Eq. (13), and listed in Table 8, have been combined with the EPGV listed in Table 6 to determine the EPGA in Table 9, for earthquakes having different Return Periods.

Interestingly, the critical EPGA results tend to be associated with small magnitude events in the near field, which is in contrast to the critical EPGD which is clearly associated with the MCE occurring in the relatively far field.

Tables 9a-9c. Effective peak ground acceleration (EPGA) predictions.

(a) 500 years return period

R(km)	M	EPGA(g's)
10	4.6	(see footnote)
20	5.3	0.23
30	5.7	0.22
50	6.3	0.21
85	7.0 (MCE)	0.13

Note: The predicted acceleration for a M=4.6 earthquake is considered to have little engineering significance and has therefore been omitted.

(b) 1000 years return period

R(km)	M	EPGA(g's)
10	5.0	0.41
20	5.6	0.31
30	6.1	0.33
50	6.8	0.29
60	7.0 (MCE)	0.24

(c) 2500 years return period

R(km)	M	EPGA(g's)
10	5.4	0.53
20	6.1	0.52
30	6.7	0.53
40	7.0 (MCE)	0.43

## 5. RESPONSE SPECTRUM MODELLING (STAGE FOUR)

5.1. Evaluation of Design Response Spectra Based on Ground Motion Parameters

Having evaluated the spectral parameters EPGD, EPGV and A/V in Stage Three above, in accordance with the seismicity and crustal conditions of the subject region (in Stages One and Two, respectively), response spectra are next developed in Stage Four to define the seismic hazard for engineering applications. A simplified procedure developed recently by the authors to determine the design response spectra may be briefly described as follows [17]. Consider the idealised displacement, velocity and acceleration response spectrum models as shown in Figure 5:

(i) Determine the displacement response spectrum for each M-R combination by identifying the EPGD, EPGV and the corresponding Corner Period T_2 as defined in Figure 5a.

(ii) Determine the acceleration response spectrum for each M-R combination by identifying the EPGV, A/V ratio and the corresponding Corner Period T_1 as defined in Figure 5c.

(iii) As an option, the velocity response spectra (Figure 5b) may be obtained from the corresponding displacement and acceleration response spectra determined in Steps (ii) and (iii), respectively.

The relationships between the idealised response spectra and the key parameters are summarised in the following (full details of their derivations have been provided [17]). The displacement response spectra can be idealised into the bi-linear form which comprises the flat part (defined by the EPGD) and the sloping part (dictated by the EPGV), as shown in Figure 5a. The corner period, T_2 , is related to EPGD and EPGV as follows:

$$T_2 = 3.14 \, EPGD / EPGV \qquad (14)$$
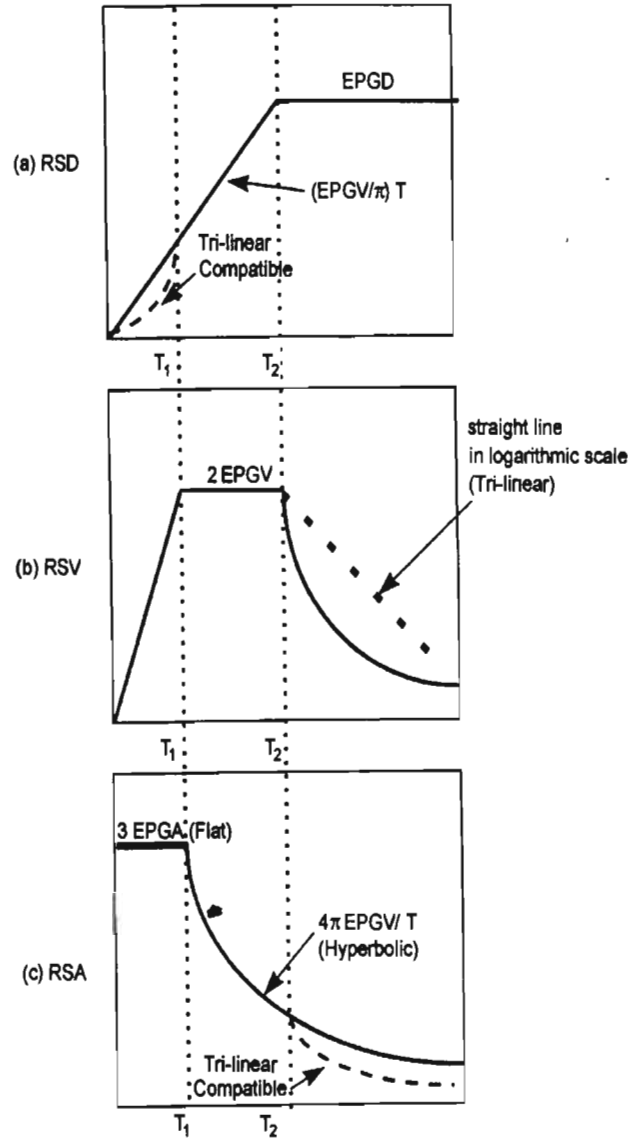
Figures 5a-5c. Idealised displacement, velocity and acceleration spectra.

(EPGD and EPGV must be in consistent SI units)

Similarly, the acceleration response spectra can be idealised into the flat-hyperbolic form which comprises the flat part (dictated by the Effective Peak Ground Acceleration, EPGA) and the hyperbolic part (dictated by the Effective Peak Ground Velocity, EPGV), as shown in Figure 5c. The corner period, T_1 , is related to A/V (EPGA/EPGV) as follows:

$$T_1 = 0.43 / (A/V) \qquad (15)$$

Note that A/V is in units of g/(m/s) in Eq. (15), and this ratio may be determined from Eq. (13).

The peak response spectral acceleration (RSA_{peak}) can be obtained from EPGV and T_1 using the following relationship:

$$RSA_{peak} = 4\pi \, EPGV / T_1 \qquad (16a)$$

Since $RSA_{peak} = 3.0 \, EPGA$ by definition [17], Eq. (16a) can be rewritten as:

$$EPGA = (4\pi/3)\,EPGV/T_1 \qquad (16b)$$

A full set of values of EPGD, EPGV, T_2, A/V, T_1 and RSA_{peak} obtained for Return Periods (T_{RP}) of 500, 1000 and 2500 years have been given in Tables 10a-10c. The corresponding Displacement and Acceleration Response Spectra are shown in Figures 6a-6c and Figures 7a-7c, respectively.

It is shown in the above tables that the EPGD parameter associated with the MCE in the far field tend to be critical for all the design Return Periods. Thus, the displacement demand predicted for the different M-R combinations with similar probability of occurrence can

deviate significantly. The EPGV parameter possesses similar trends, but the differences are much less pronounced. Interestingly, this trend is reversed in the high frequency parameters such as the RSA_{peak}. In theory, RSA_{peak} associated with the small magnitude events are most critical due to the magnitude dependent A/V ratios. However, the arbitrarily defined minimum corner period of 0.1 (T_1) seconds in Table 10 has significantly capped its value for smaller M-R combinations. Consequently, both the displacement and acceleration response spectra associated with the MCE combinations are generally more critical than those associated with the other M-R

Table 10a. Response spectrum parameters for 500 years return period.

M	R km	EPGD mm	EPGV mm/sec	T_2 secs	A/V g/(m/sec)	T_1 secs	RSA_{peak} g's
5.3	20	5	32 ·	0.52	7.2	0.10 (.06)	0.41
5.7	30	8	35	0.70	6.4	0.10 (.07)	0.44
6.3	**50**	14	42	**1.05**	**4.9**	**0.10 (.09)**	**0.54**
7.0 (MCE)	85	20	46	**1.39**	**2.8**	**0.15**	**0.38**

Table 10b. Response spectrum parameters for 1000 years return period.

M	R km	EPGD mm	EPGV mm/sec	T_2 secs	A/V g/(m/sec)	T_1 secs	RSA_{peak} g's
5.0	10	8	53	0.50	7.9	0.10 (.05)	0.67
5.6	20	9	46	0.65	6.8	0.10 (.06)	0.59
6.1	30	17	56	0.94	5.9	0.10 (.07)	.0.72
6.8	**50**	28	67	**1.30**	**4.3**	**0.10**	**0.85**
7.0 (MCE)	**60**	29	65	**1.39**	**3.7**	**0.12**	**0.72**

Table 10c. Response spectrum parameters for 2500 years return period.

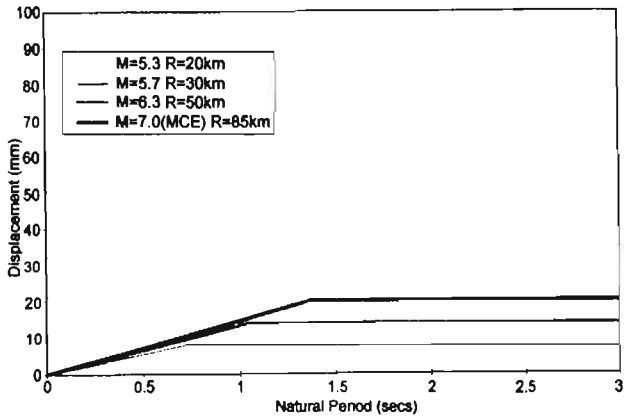| M	R km	EPGD mm	EPGV mm/sec	T_2 secs	A/V g/(m/sec)	T_1 secs	RSA_{peak} g's
5.4	10	12	71	0.55	7.4	0.10 (.06)	0.91
6.1	20	25	84	0.94	6.2	0.10 (.07)	1.08
6.7	30	41	102	**1.25**	**5.2**	**0.10 (.08)**	**1.31**
7.0 (MCE)	**40**	43	98	1.39	4.4	0.10	1.29

Figure 6a. Displacement response spectra for 500 years return period.

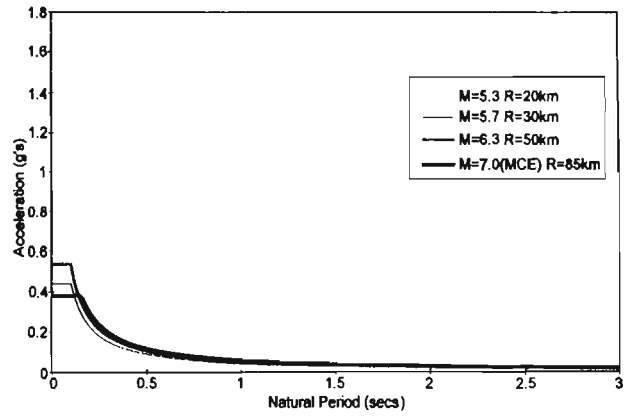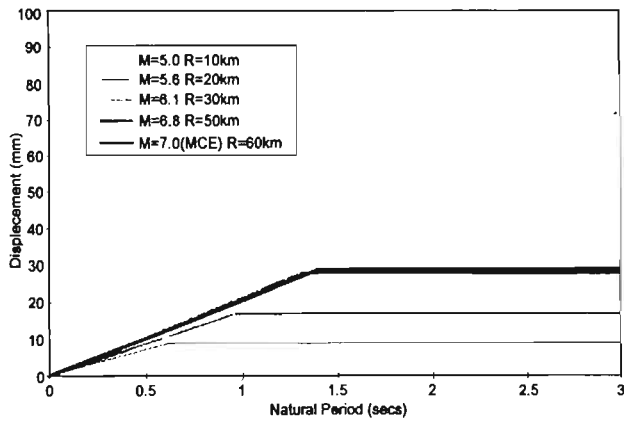**Figure 7a.** Acceleration response spectra for 500 years return period.

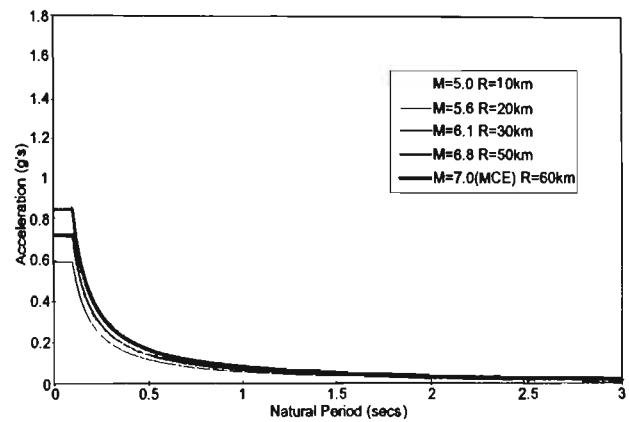**Figure 6b.** Displacement response spectra for 1000 years return period.

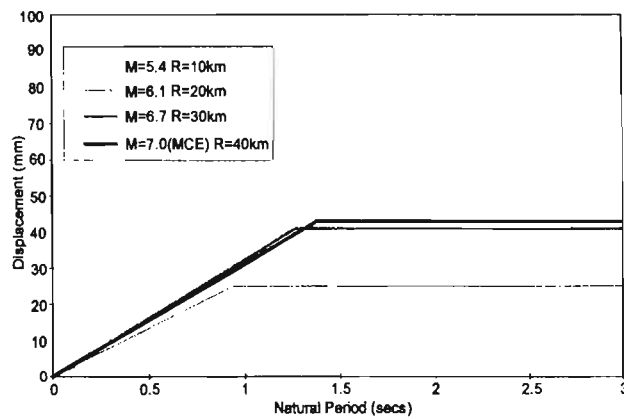**Figure 7b.** Acceleration response spectra for 1000 years return period.

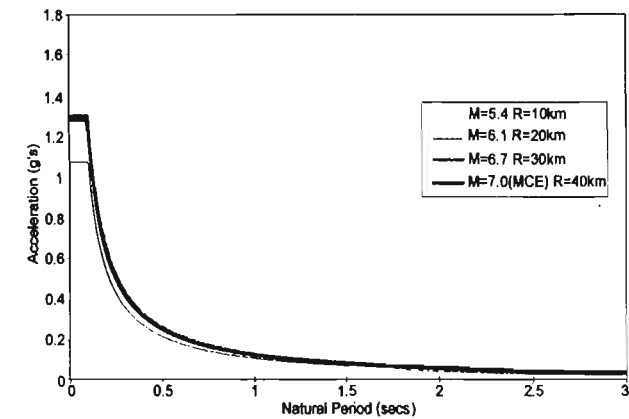**Figure 6c.** Displacement response spectra for 2500 years return period.

Figure 7c. Acceleration response spectra for 2500 years return period.

combinations, within the period range of engineering interest. Thus, the magnitude (M) assumed for the MCE (M7.0 in this study) is often critical. The determination of the MCE is further discussed in the second part of the paper [9].

5.2. Comparisons with Scott Recommendation and the Chinese Earthquake Design Code (CRSC Region)

A 1000 year Return Period design response spectrum model has been proposed by Scott et al [4] for rock sites in Hong Kong (which is located within the CRSC region). Importantly, the response spectrum predicted by Scott in the medium period range is in very good agreement with the predictions in this study based on the generic crustal model, as shown in Figures 8a and 8b. The good agreement in the two response spectrum models was expected since both models were originally developed from earthquake ground motion data and attenuation relationships for events recorded in ENA. However, there are noticeable discrepancies in other period ranges. The
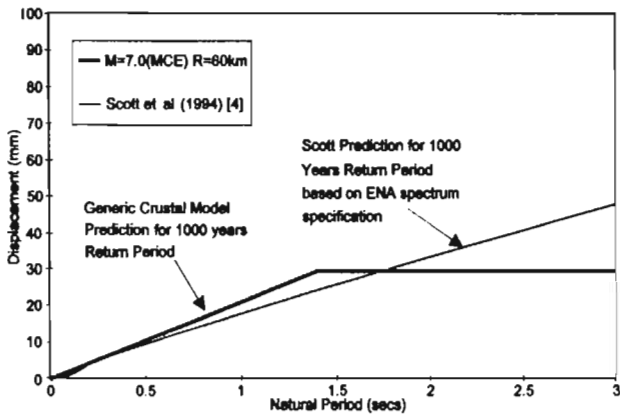
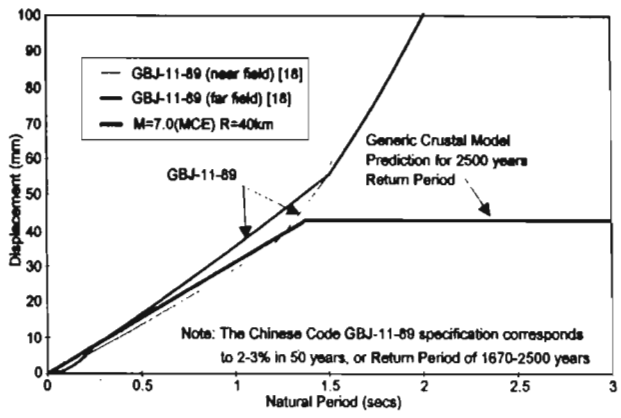**Figure 8a.** Comparison of displacement response spectra for 1000 years return period.

Figure 9a. Comparison of displacement response spectra for 2500 years return period.
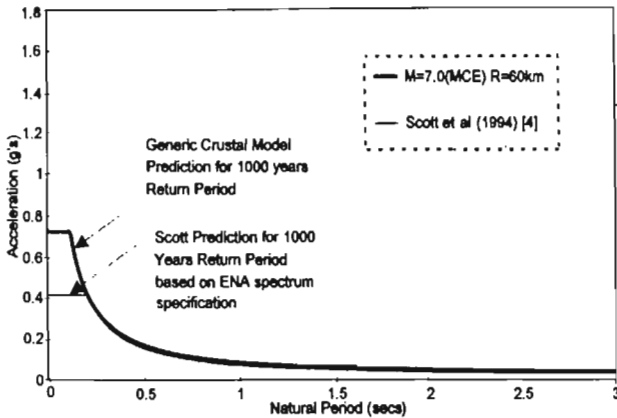

Figure 8b. Comparison of acceleration response spectra for 1000 years return period.
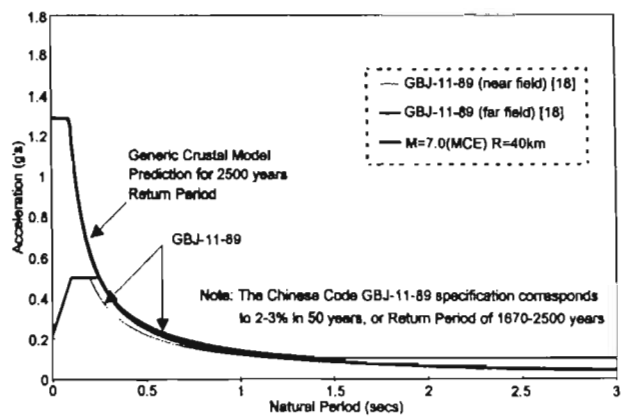

Figure 9b. Comparison of the acceleration response spectra for 2500 years return period.

discrepancy in the long period range is a result of the omission of the second corner period (T_2) in the Scott model (see Figure 8a), whereas the discrepancy in the short period range is a result of the different assumed first corner period (T_1) (see Figure 8b). The latter difference implies an A/V ratio in the Scott et al [4] model of approximately 2.0, which is significantly lower than values quoted for the generic "Hard Rock" model in Table 8.

Response spectrum predictions obtained using the generic crustal model have been further compared with current code recommendations (see Figures 9a and 9b). The Chinese earthquake design code [18] stipulates the CRSC to be in a zone of Intensity degree VII (seven). This is associated generally with an effective peak ground acceleration (EPGA) for a major (very long return period) earthquake in the order of 0.22g, which is considerably lower than that predicted in this paper (Table 9) although such values are in good agreement with empirical PGA predictions [7], as discussed in Reference [9]. It is noted that the Chinese code design spectrum (assuming a stiff soil site of Type I, as the code does not consider rock sites independently) for a major earthquake requiring ultimate limit state design is associated with a probability of occurrence in the order of 2-3% in 50 years [34], giving an average return period of about 1700-2500 years, the

highest value of this range being also considered in this paper (see Figure 9). For the CRSC, the code stipulates two design response spectra, corresponding to "near" and "distant" earthquake events. The distinction affects only the corner period T_1, which takes the values 0.2sec and 0.25sec, respectively (see Figures 9a-9b). The near earthquake is considered to be an event producing a maximum (epicentral) intensity I_0 of 9 or above [18]. These conditions may be related to earthquake magnitude (M), using an empirical magnitude-intensity relationship for South China. Such a relationship has been obtained using an elliptical attenuation model, based on historical earthquake intensity data compiled for the South China region [1], as follows:

$$M = 0.76I_0 - 0.60 \qquad (17)$$

For the near event and using Eq. (17), the magnitude should not exceed M=5.5 and for the distant event, M should be 6.25 or larger. These values may be related to the design M-R combinations of this paper, as summarised in Table 3a. For example, when the design return period is taken as 1000 years, the event at R=20km is at the limit of the "near field", whereas events at $R > 35km$ (approximately) would be considered as "far field".

It is noted from Figures 9a and 9b that the response

spectra specified by the Chinese code and those predicted by this study based on similar return periods are in very good agreement in the medium period range. Discrepancies in other period ranges are similar to those shown in Figures 8a and 8b, and the reasons for these discrepancies have been briefly explained above. The long-period discrepancy between the Chinese code spectrum and the seismological model prediction, which is especially evident in Figure 9a, is due mainly to the stipulation by the code of a minimum design spectral acceleration of 0.1g (20% of the peak spectral acceleration), for periods above around 1.5 seconds (see Figure 9b).

6. CONCLUSIONS

❖ A procedure to determine the seismic hazard of the Coastal Region of South China (CRSC), based on the assumption of uniform seismicity, has been introduced within the framework of a seismological model. The procedure has been developed in four major Stages.

❖ In Stage One, the seismicity of the CRSC has been reviewed based on a number of magnitude-recurrence relationships derived previously for the subject region. Critical, probabilistically-based magnitude-distance (M-R) combinations have been derived for near and far field events, taking a range of design return periods from 500 to 2500 years.

❖ In Stage Two, the contributions made by the earthquake source to the key displacement and velocity ground motion parameters have been presented in accordance with generic source model. In carrying out this analysis, a generic (as opposed to regional) crustal classification was adopted, based directly on the crustal conditions pertaining in Eastern North America (ENA).

❖ In Stage Three, the peak ground motions (displacement EPGD, velocity EPGV and acceleration EPGA) and corresponding key ground motion ratios such as A/V (EPGA/EPGV) have been predicted, for design return periods ranging between 500 and 2500 years, and assuming the simplified generic source and crustal models. The ground motion ratios predicted using the seismological model are in general agreement with expectations based on a small number of actual strong-motion recordings in moderate seismicity regions such as Canada and Australia.

❖ In Stage Four, the displacement, velocity and acceleration response spectra were derived in accordance with the predicted peak ground motion parameters.

❖ Design response spectra predictions made using the seismological model (based on critical M-R combinations) were found to be very consistent with current code provisions, and with design spectra proposed by other researchers, in the

velocity controlled medium period range. However, significant discrepancies have been identified in other period ranges.

❖ The ground motion parameters and response spectra derived in this study were based on the generic ENA crustal conditions. The effects the regional crustal properties and the crustal thickness have upon the ground motion parameters have been described in the second part of the paper [9].

REFERENCES

1. Lee, C.F., Ding, Y., Huang, R., Yu, Y., Guo, G., Chen, P., and Huang, X. (1996). "Seismic Hazard Analysis of the Hong Kong Region", Geotechnical Engineering Office, Civil Engineering Department, Hong Kong SAR Government (GEO Report No. 65).

2. Chandler, A.M., and Lee, C.F. (1999). "Seismic Hazard Review of the Hong Kong Region", *Proceedings of the Workshop on Earthquake Engineering for Regions of Moderate Seismicity*, Hong Kong Special Administrative Region, China.

3. Wong, Y.L., Zhao, J.X., Chau, K.T., and Lee, C.M. (1998). "Assessment of Seismicity Model for Hong Kong Region", *Transactions for Hong Kong Institution of Engineers*, 5(1), 50-62.

4. Scott, D.M., Pappin, J.W., and Kwok, M.K.Y. (1994). "Seismic Design of Buildings in Hong Kong", *Transactions of the Hong Kong Institution of Engineers*, 1(2), 37-50.

5. Pun, W.K., and Ambraseys, N.N. (1992). "Earthquake Data Review and Seismic Hazard Analysis for the Hong Kong Region", *Earthquake Engineering and Structural Dynamics*, 23, 433-443.

6. Cornell, C.A. (1968). "Engineering Seismic Risk Analysis", *Bulletin of the Seismological Society of America*, 58, 1583-1606.

7. Huo, J., Hu, Y., and Feng, Q. (1992). "Study on Estimation of Ground Motion from Seismic Intensity", *Earthquake Engineering and Engineering Vibration*, 12(3), 1-15.

8. Tian, Q., Liao, Z., and Sun, P. (1986). "Estimation of Ground Motion Attenuation in China Based on Intensity Data", *Earthquake Engineering and Engineering Vibration*, 6(1), 21-36.

9. Lam, N.T.K., Chandler, A.M., Wilson, J.L., and Hutchinson, G.L. (1999). "Seismic Hazard Determination for the Coastal Region of South China II: Region Crustal Modelling", *Journal of Seismology and Earthquake Engineering* (in press).

10. Atkinson, G. (1993). "Earthquake Source Spectra in Eastern North America", *Bulletin of the Seismological Society of America*, 83, 1778-1798.

11. Beresnev, I.A., and Atkinson, G.M. (1997). "Modelling Finite-Fault Radiation from the ω^n Spectrum", *Bulletin of the Seismological Society of America*, 87(1), 67-84.

12. Atkinson, G., and Silva, W. (1997). "An Empirical Study of Earthquake Source Spectra for California Earthquakes", *Bulletin of the Seismological Society of America*, 87, 97-113.

13. Atkinson, G.M., and Boore, D.M. (1998). "Evaluation of Models for Earthquake Source Spectra in Eastern North America", *Bulletin of the Seismological Society of America*, 88(4), 917-934.

14. Lam, N.T.K., Wilson, J.L., and Hutchinson, G.L. (1998). "Development for Intraplate Response Spectra for Bedrock in Australia", *Proceedings of the 1998 Technical Conference of the New Zealand National Society for Earthquake Engineering*, Wairakei, 27-29.

15. Lam, N.T.K., Wilson, J.L., and Hutchinson, G.L. (1999). "Generation of Synthetic Earthquake Accelerograms Based on the Seismological Model: A Review", *Journal of Earthquake Engineering* (in press).

16. Lam, N.T.K., Wilson, J.L., and Hutchinson, G.L. (1999). "A Generic Displacement Spectrum Model for Rock Sites in Low Seismicity Regions", *Journal of Earthquake Engineering* (under review).

17. Lam, N.T.K., Wilson, J.L., Chandler, A.M., and Hutchinson, G.L. (1999). "Response Spectrum Modelling in low and Moderate Seismicity Regions Combining Velocity, Displacement and Acceleration Predictions", *Earthquake Engineering and Structural Dynamics* (under review).

18. Ministry of Construction of the People's Republic of China (1994). "Code for Seismic Design of Buildings", National Standard of the Peoples's Republic of China GBJ 11-89.

19. Jacob, K.H. (1997). "Scenario Earthquakes for Urban Areas ·Along the Atlantic Seaboard of the United States", NCEER-SP-0001, National Centre for Earth-

quake Engineering Research, Buffalo, New York.

20. Reiter, T. (1990). *"Earthquake Hazard Analysis"*, Columbia University Press, New York.

21. Yeats, R.S., Sieh, K., and Clarence, R.A. (1997). *The Geology of Earthquakes*, Oxford University Press, New York and Oxford.

22. Chan, L.S., and Zhao, A. (1996). "Frequency and Time Series Analysis of Recent Earthquakes in the Vicinity of Hong Kong", *Hong Kong Geologist*, 2, 11-19.

23. Boore, D.M. (1986). "Short-Period P- and S-Wave Radiation from Large Earthquakes: Implications for Spectral Scaling Relations", *Bulletin of the Seismological Society of America*, 76(1), 43-64.

24. Boore, D.M., and Joyner, W.B. (1997). "Site Amplification for generic Rock Sites", *Bulletin of the Seismological Society of America*, 87(2), 327-341.

25. Wilkie, J., and Gibson, G. (1995). "Estimation of Seismic Quality Factor Q for Victoria, Australia", *AGSO Journal of Geology and Geophysics*, 15(4), 511-517.

26. Bureau of Geology and Mineral Resources of Guangdong Province (1982). "Regional Geology of Guangdong Province", *Geological Publishing House, Beijing*, Series 1, No. 9.

27. Clark, I.F., and Cook, B.J. (1983). "Geological Science: Perspectives of the Earth", Copyright: Australian Academy of Science, Canberra.

28. Feng, R., Zhu, J., Ding, Y., Chen, G., He, Z., Yang, S., Zhou, H., and Sun, K. (1981). "Crustal Structure in China from Surface Waves", *ACTA Seismological Sinica*, 3(4), 336-350.

29. Ambraseys, N.N., Simpson, K.A., and Bommer, J.J. (1996). "Prediction of Horizontal Response Spectra in Europe", *Earthquake Engineering and Structural Dynamics*, 25, 371-400.

30. Bommer, J.J., And Elnashai, A.A. (1998). "Parameterised Displacement Spectra for Seismic Design". Engineering Seismology and Earthquake Engineering Research Report No. 98-7, Civil and Environmental Engineering Department, Imperial College of Science, Technology and Medicine, London.

31. Atkinson, G.M., and Boore, D.M. (1995). "Ground-Motion Relations for Eastern North America", *Bulletin of the Seismological Society of America*, 85(1), 17-30.

32. Chandler, A.M. (1991). "Evaluation of Site-Dependent Spectra for Earthquake-Resistant Design of Structures in Europe and North America", *Proceedings of the Institution of Civil Engineers*, Part 1, 605-626.

33. Tso, W.K., Zhu, T.J., and Heidebrecht, A.C. (1992).

"Engineering Implication of Ground Motion A/V Ratio", *Soil Dynamics and Earthquake Engineering*, 11, 133-144.

34. Hu, S. (1993). "Seismic Design of Buildings in China", *Earthquake Spectra*, 9(4) 703-737.